MeerKAT: some investigations of the layout.

I M Stewart

April 16, 2011

1 Introduction

These investigations were prompted firstly by a concern that the distribution of Meerkat antennas looked flattened in a north-south direction; secondly because the material in section 3.3 of M0000-0000V1-11 TM(D), the requirements analysis for spectral line use cases, appeared to be not completely self-consistent.

One slight caveat: I did most of this in two days, so there are almost certainly some mistakes here. (This whole topic is in need of some care and time in my opinion.) For example in the plots in section 2 I have taken no particular care to adhere to conventions respecting axis directions and position angle origin and sign. Some flips and inversions may well be necessary to align them with convention.

2 Array layout issues

2.1 Sources

Antenna locations for Meerkat have been calculated by Bradley Frank using 'AntConfig', a software package for array layout optimization written by Mattieu de Villier. I am told that all calculations of array positions are performed by AntConfig in the WGS84 coordinate system, these positions being subsequently converted to ENU.

WGS84 is a coordinate system based on the earth reference ellipsoid. Coordinates are geodetic latitude, geodetic longitude (which is offset by a few arcsec from the geocentric value), and height above the ellipsoid surface. A 'geoid' representing the approximate surface of mean sea level is defined 'on top of' the ellipsoid as part of the WGS84 standard, but this is not relevant to the present purpose. ENU stands for East North Up and is a Cartesian system with axes in a plane tangent to the geoid at some reference location (in the present case this is taken to be the average position of the antennas). These systems are described at

`http://en.wikipedia.org/wiki/World_Geodetic_System`
`http://en.wikipedia.org/wiki/Geodetic_system`

I obtained a file giving ENU positions of the antennas, with the latitude and longitude of the reference point being given as -30.71317 and 21.44389 respectively. More recently I obtained a file giving WGS84 locations from Jasper Horrell.

2.2 Broad effects

I was concerned about the north-south flattening I seemed to see in a plot of the antenna locations. Calculation of the standard deviation of north vs east displacements returned 940 m

for the north standard deviation vs. 1167 m for the east, confirming that the effect is real. A very rough initial calculation suggested the ratio is equal to cos(-31=Meerkat latitude), strongly suggesting a numerical error, but when I took more care I found that this is in fact not true to any plausible accuracy.

I wrote a script to encode my own conversion from WGS84 to ENU, using formulae from

`http://en.wikipedia.org/wiki/Geodetic_system`

The results were interesting. My ENU antenna positions came out the same as the supplied ENU positions except that mine are displaced east by 60 m and south by 79 m. The north-south 'squash' is preserved however.

Should the spread of the array to the north and east be the same - i.e. is it desirable that it have approximate azimuthal symmetry? Complicated question. The transformation from array layout to an earth-rotation aperture synthesis (ERAS) baseline distribution involves an auto-correlation followed by 3D rotational smearing followed by projection toward the phase centre. A circularly-symmetric array is only guaranteed to return circularly-symmetric ERAS baselines at all declinations if it is situated on the equator. Perhaps there is reason to squash the array north-south somewhat but I have not seen this reason documented. I would have thought it was better to stretch the layout slightly in the N-S direction rather than squash it.

I note finally that *geodetic* latitude is not the same as the *geocentric* or true latitude. A look at the supplied file of WGS84 positions shows that the average geodetic latitude of the antennas is very close to the figure of -30.71317 supplied as the reference latitude (presumably geocentric) of the ENU positions. The true latitude of the array centre as given by the WGS84 positions is about -30.54 degrees, some 19 km further north.

2.3 Fine details

I was interested to look at the distribution of baselines for a zenith snapshot. In a sense this displays the array both at its worst and at its best at the same time: worst because one gains no smoothing benefit from ERAS; best because there is no flattening due to mismatch between the array latitude and the declination of the pointing centre.

In order to avoid effects due to the north-south flattening observed in section 2.2 I multiplied the north-south displacements from centre by 1.24 before doing the calculations and plots in the remainder of the report.

Figure 1 shows a histogram of the baseline magnitudes (or radii). It can be seen that its smoothness appears not to be optimum. I cannot think that the hump around 4 km serves any purpose. A direct plot of the baseline locations also reveals an azimuthal unevenness (figure 2), although this is smoothed out to some degree if the Hermitian conjugate positions are added (figure 3).

The bunching is typically caused by a small subset of antennas (see for example figures 4 and 5) and could therefore be substantially improved by relocating only a small number of antennas.

3 Sensitivity at different resolutions

R.U.P045 as quoted at the head of section 3.3 of M0000-0000V1-11 TM(D), the requirements analysis for spectral line use cases, mandates that the sensitivity of the interferometer at L band, *with natural weighting*, should change by no more than 25% for angular scales from 8 to 80 arcsec, under certain conditions of declination and duration. Figure 5 in this section appears

to display RMS noise in the dirty image for a range of taper widths. Questions and objections arising here are

- The RUP demands natural weighting, but the figure applies tapered weights.
- What exactly is meant by 'sensitivity'?
- What exactly is meant by 'angular scale'?

Two separate but related ways occur to me in which one might think about sensitivity. Each carries with it certain obvious interpretations of 'angular scale'.

1. What is the noise RMS at various spatial scales, and/or under various weighting schemes?
2. How bright will a source of a given width appear in Meerkat dirty images?

These are related because weighting will affect the signal strength as well as the noise. Indeed filter theory suggests that an optimum weight function will have the same shape as the signal (matched filter).

The amount of noise power at different spatial scales for natural weighting is given trivially by the histogram in figure 1. If instead one considers non-natural weighting, a figure of (de)merit ρ_{noise} for noise is the ratio of noise RMS in the dirty image to that produced with natural weighting. (Given a point source, and equal noise temperatures on all visibilities, natural weighting is well known to give rise to the lowest noise RMS.) It is not hard to work out, or you can obtain it from a number of sources, eg Wrobel and Walker [1999], that this ratio is given by

$$\rho_{\text{noise}} = \frac{\sqrt{N \sum_k^N W^2(u_k, v_k)}}{\sum_k^N W(u_k, v_k)}$$

where $W(u_k, v_k)$ is the weight at (u_k, v_k) and N is the number of visibilities.

There are endless ways to generate visibility weights but I restrict myself just to combinations of density weights and Gaussian taper weights of the form

$$W_{\text{taper}}(u, v) = \exp\left[\frac{-(u^2 + v^2)}{2\sigma^2_{\text{taper}}}\right]. \tag{1}$$

Note that Gaussian tapering in the UV plane is equivalent to a convolution in the image plane by the Fourier inverse of W_{taper}. This inverse is also of course a Gaussian with a sigma $\sigma_{\text{convolver}}$ (in radians) equal to $1/2\pi\sigma_{\text{taper}}$ (in waves).

The first thing I did was attempt to reproduce figure 5 of M0000-0000V1-11 (I'll refer to this as M.5 for short) by plotting ρ_{noise} against $\sigma_{\text{convolver}}$ - see figure 6. I found I could duplicate the shape of the plot pretty well if I constructed my weights by dividing the taper weight by the density of visibility samples ($\rightarrow$ tapered uniform weighting). It is of course nontrivial to estimate sample densities, one has either to grid or to use Mattieu's Voronoi tessalation approach. I just constructed a histogram of the baseline radii as in section 2.3 and divided the numbers in each bin by the area of the corresponding annulus.

Note however that to get the dip in my graph to line up with the dip in figure M.5 I had to multiply my taper widths by π. There appears also to be a factor of 2 vertical scaling difference which I have not corrected. Considering the haste with which I constructed this figure, it is not just possible but probable that the source of these discrepancies is my own error. Nevertheless, it is a thing which needs to be accounted for by someone with more time to spend on it.

If one asks instead question 2, well there are two ways one might want to frame it. We might ask, given a source brightness distribution $f(l,m)$ with a Gaussian shape and total flux density S, located at the phase centre:

$$f(l,m) = \frac{S}{2\pi\sigma^2} \exp\left[\frac{-(l^2+m^2)}{2\sigma^2_{\text{source}}}\right],$$

what will be the 'janskys per beam' at the centre of the dirty image? Or better, what will be the ratio between this central brightness and that of a point source with the same flux density? This ratio ρ_{signal} is given by

$$\rho_{\text{signal}} = \frac{\sum_k^N F(u_k,v_k) \times W(u_k,v_k)}{F(0,0)\sum_k^N W(u_k,v_k)}$$

where F is the real part of the (in any case real-valued here) Fourier transform of the source brightness distribution.

An obvious candidate for an overall figure of merit is the ratio between ρ_{signal} and ρ_{noise}. This value is plotted in figure 7 for a range of values of both the source and convolver widths up to 100 arcsec.[1] The conjecture that the optimum taper matches that of the source is confirmed.

This is not entirely satisfactory because the central value of a Gaussian profile of constant volume naturally decreases proportional to 1 over sigma squared. The human eye does pretty well at integrating flux however, thus a broad and a narrow source of the same flux density may in practice be about equally visible against the noise floor. So it is of interest to consider an alternative case in which the source central brightness is held constant. It is difficult to be so neatly systematic in this case - one cannot compare to an infinitely narrow source of the same central brightness because such a point source would have zero total flux density. However, a rough idea of source visibility can arguably be obtained by multiplying the values in figure 7 by the square of the source width σ_{source}. The vertical scale becomes arbitrary because, as said, there is no ratio involved. All it does is give an idea of how source visibility might vary as a function of σ_{source} and $\sigma_{\text{convolver}}$. This adjusted figure is given in figure 8.

The visibility is clearly still rising at $\sigma_{\text{source}} = 100$ arcsec. But since the maximum occurs when the taper convolver has the same width, there is no point really in pursuing these 2D plots further. A section through figure 8 along the 45° maximal line is shown in figure 9. This at least shows that larger and larger sources don't keep getting more visible indefinitely. The requirement specified natural weighting though, so this is presented in figure 10. (This graph is a slice through figure 8 at the $\sigma_{\text{convolver}} = 0$ line.) This looks a bit flatter for ranges of σ_{source} which are closer to the size scale of the requirement.

In the end, neither the central-flux nor total-flux measures seems entirely satisfactory. A program of simulations plus human-eye detection experiments would be good to calibrate this important criterion.

4 Conclusions

The array layout as given is compressed north-south by a factor of approximately 1.24. I am not aware of any reason for this and my guess is that it is probably undesirable.

The array central latitude given in the ENU file appears to be a geodetic value, whereas the normal assumption would be that it is a geocentric or true value. If taken as a true value, the

[1] NOTE that uniform weighting was NOT applied in the generation of figures 7 through to 10 - i.e. the Gaussian taper W_{taper} given in equation 1 was all that was used here.

array centre will end up 19 km north of the position used in the calculations. Unless care is taken this could also have the effect of displacing the antenna ENU locations vertically by up to 10 metres at the northern- and southernmost extremities of the array. In practice of course neither of these is likely to cause serious error, since the array centre will be dictated by geography and the antenna heights by the local terrain; the most important thing is the list of horizontal offsets from centre. Nevertheless such loose ends are undesirable as potential sources of confusion and error.

The azimuthal smoothness of the antenna distribution is suboptimum. Although this is likely only of importance for snapshot observations, it would nevertheless be quite easy to improve it by shifting a small number of antennas.

The Meerkat array layout is meant to be optimized to be sensitive to HI over a broad range of size scales. Figure M.5 of M0000-0000V1-11 TM(D) could be reproduced in qualitative terms, which increases confidence in the results obtained from AntConfig. Scale inconsistencies remain on both axes however and the sources of these need to be tracked down. It also appears that figure M.5 was obtained by tapered uniform weighting, which is far from the natural weighting the specification requires. Either the specification should be modified or some different criterion for sensitivity at varying resolution should be adopted.

The somewhat ragged distribution of baseline lengths also tends to suggest the optimization is not perfect.

Acknowledgements

Thanks to my current, temporary boss Huib van Langeveld for being a good bloke in general, and for acquiescing to me stealing JIVE time to look into Meerkat problems in particular.

References

[1999] Wrobel J. M. & Walker R. C. 1999, "Synthesis Imaging in Radio Astronomy II", ASP Conf. Ser. 180, 171-186

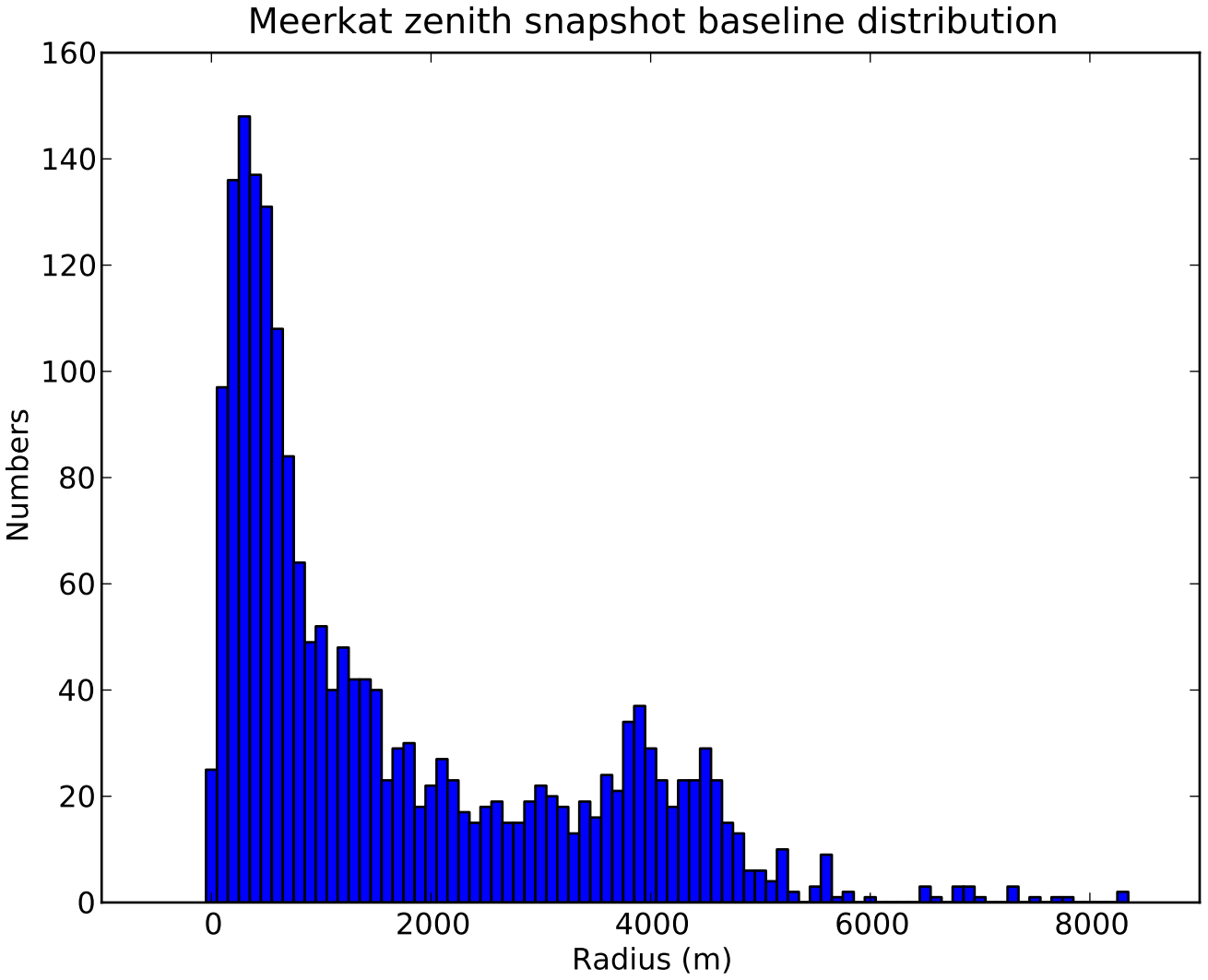


Figure 1: Distribution of Meerkat baselines.

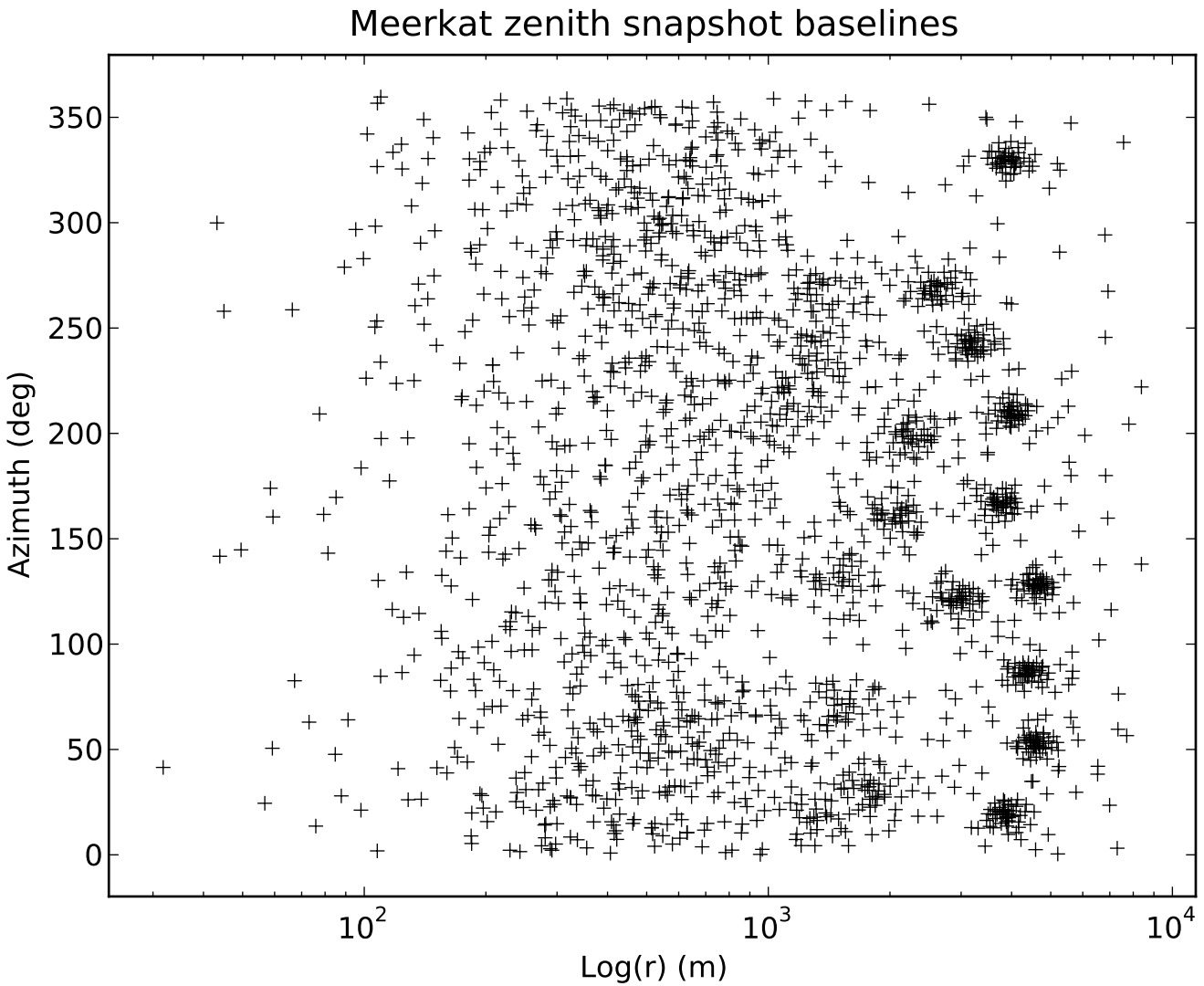


Figure 2: Meerkat baselines.

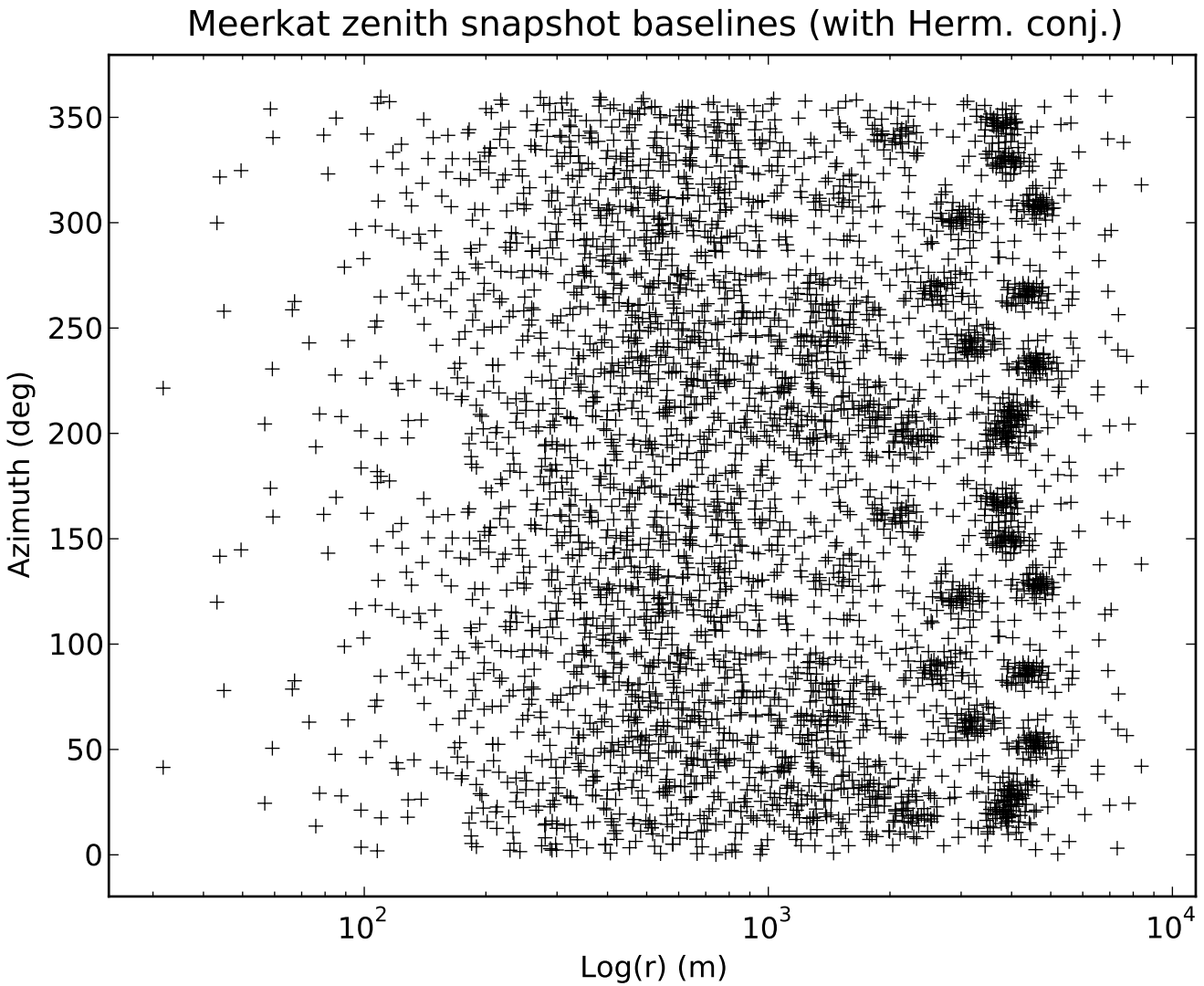


Figure 3: Meerkat baselines, including Hermitian conjugates.

Figure 4: Distribution of Meerkat baselines with those including antenna 53 (counting from 0) highlighted.

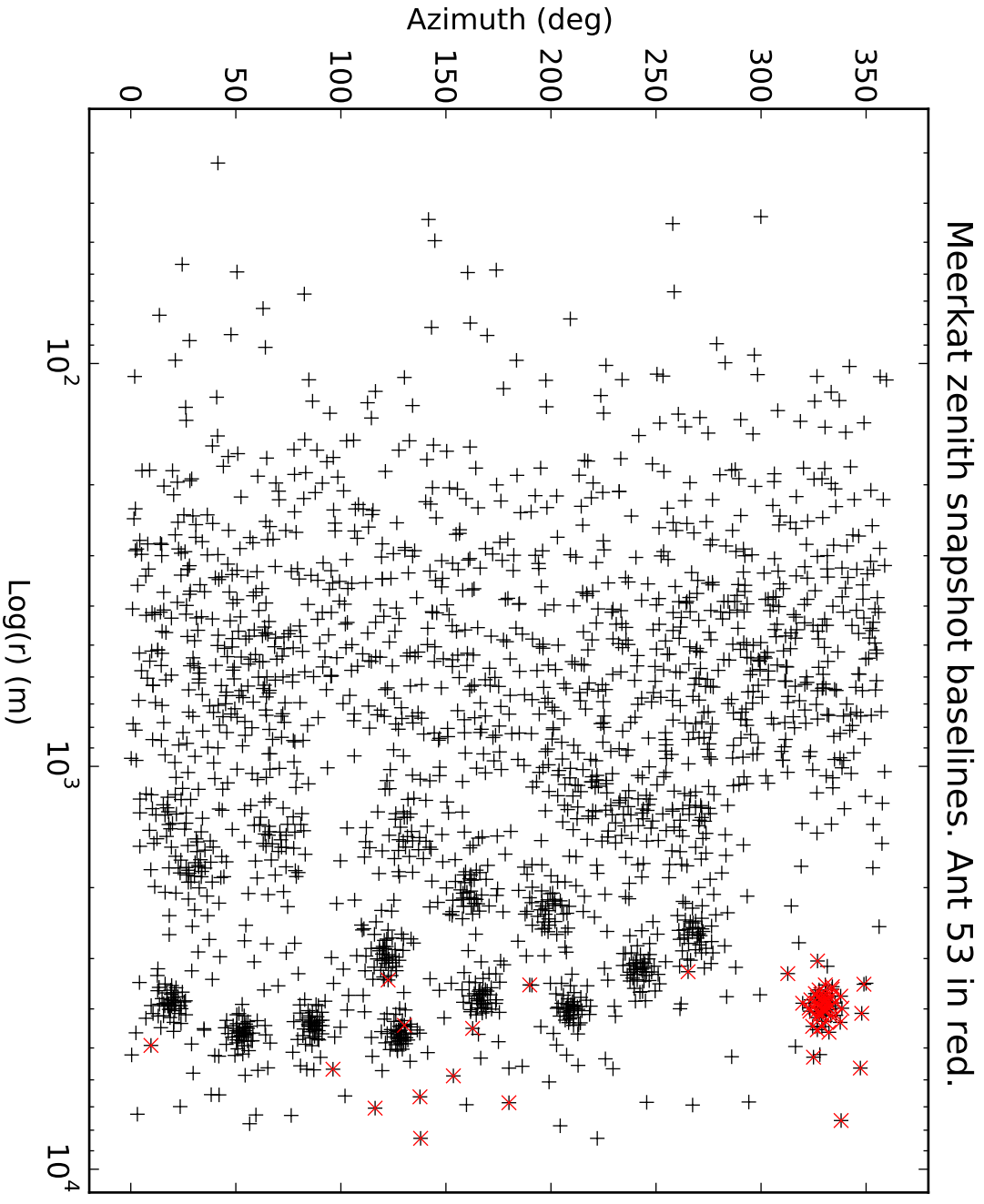


Figure 5: Meerkat baselines with those including antenna 53 (counting from 0) highlighted.

Figure 6: Log-log plot of noise ratio versus taper width for tapered quasi-uniform weighting.

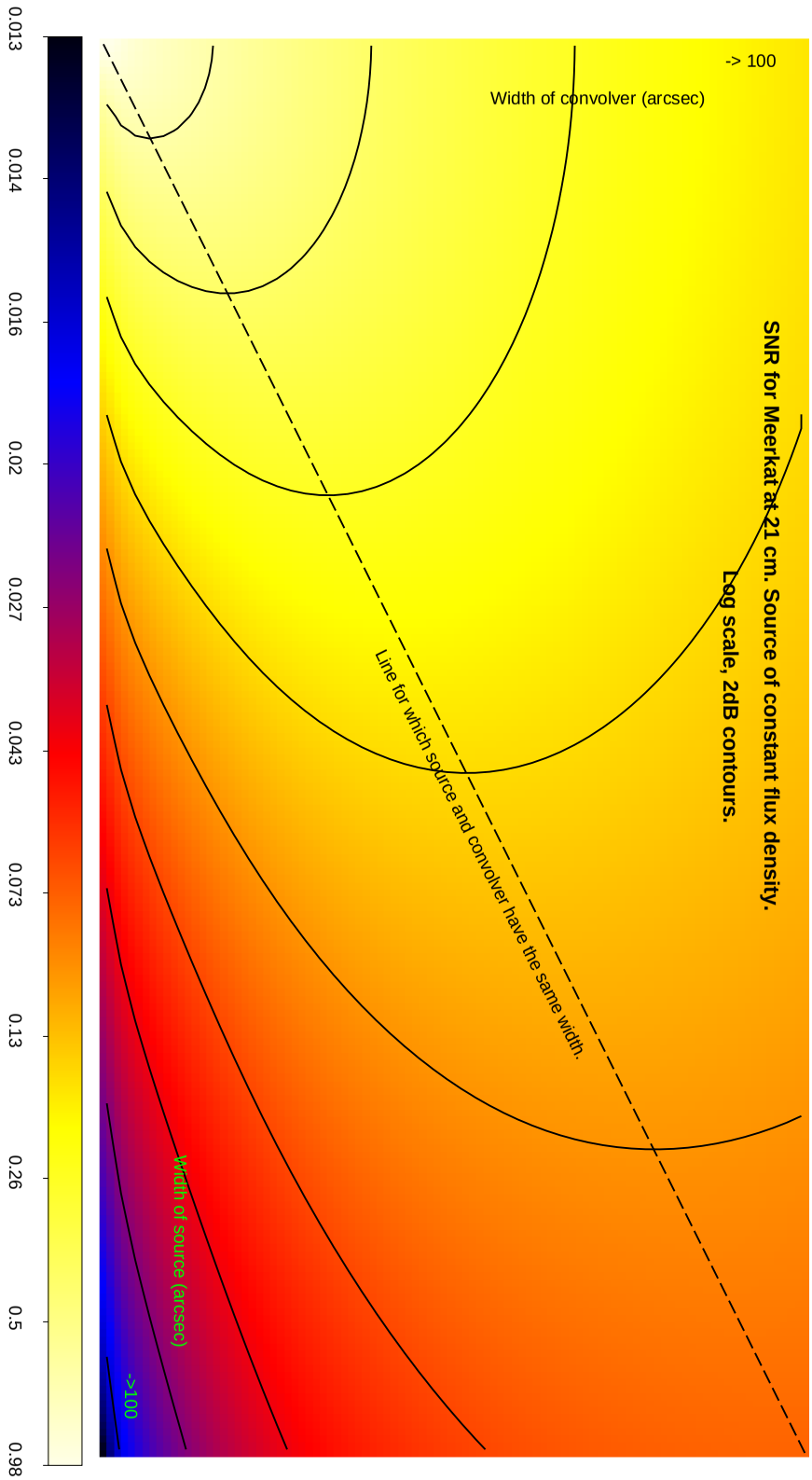


Figure 7: Source relative central brightness at different widths and tapers.

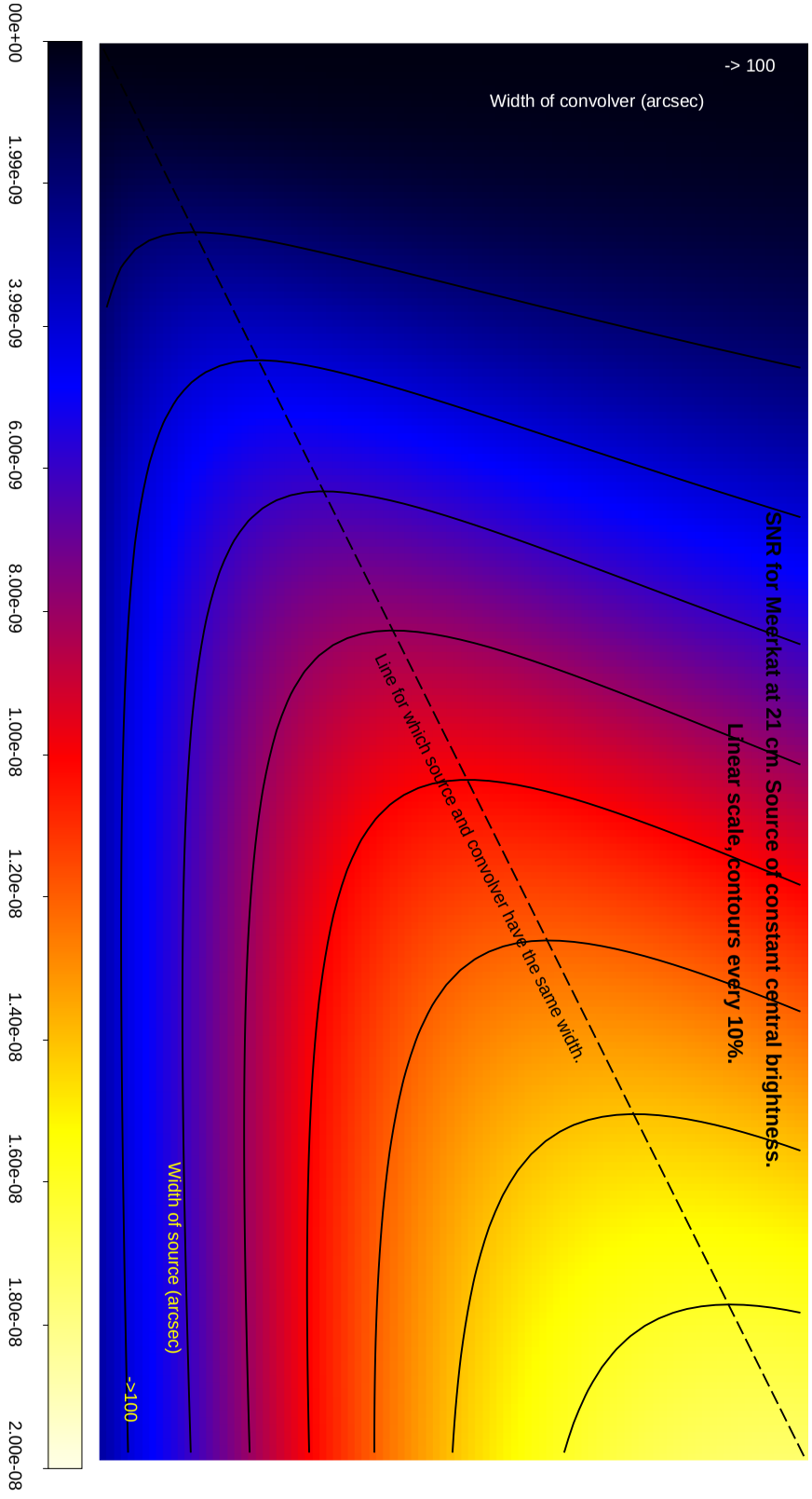


Figure 8: Source 'visibility' at different widths and tapers.

Figure 9: Source 'visibility' for matched-tapered weighting.

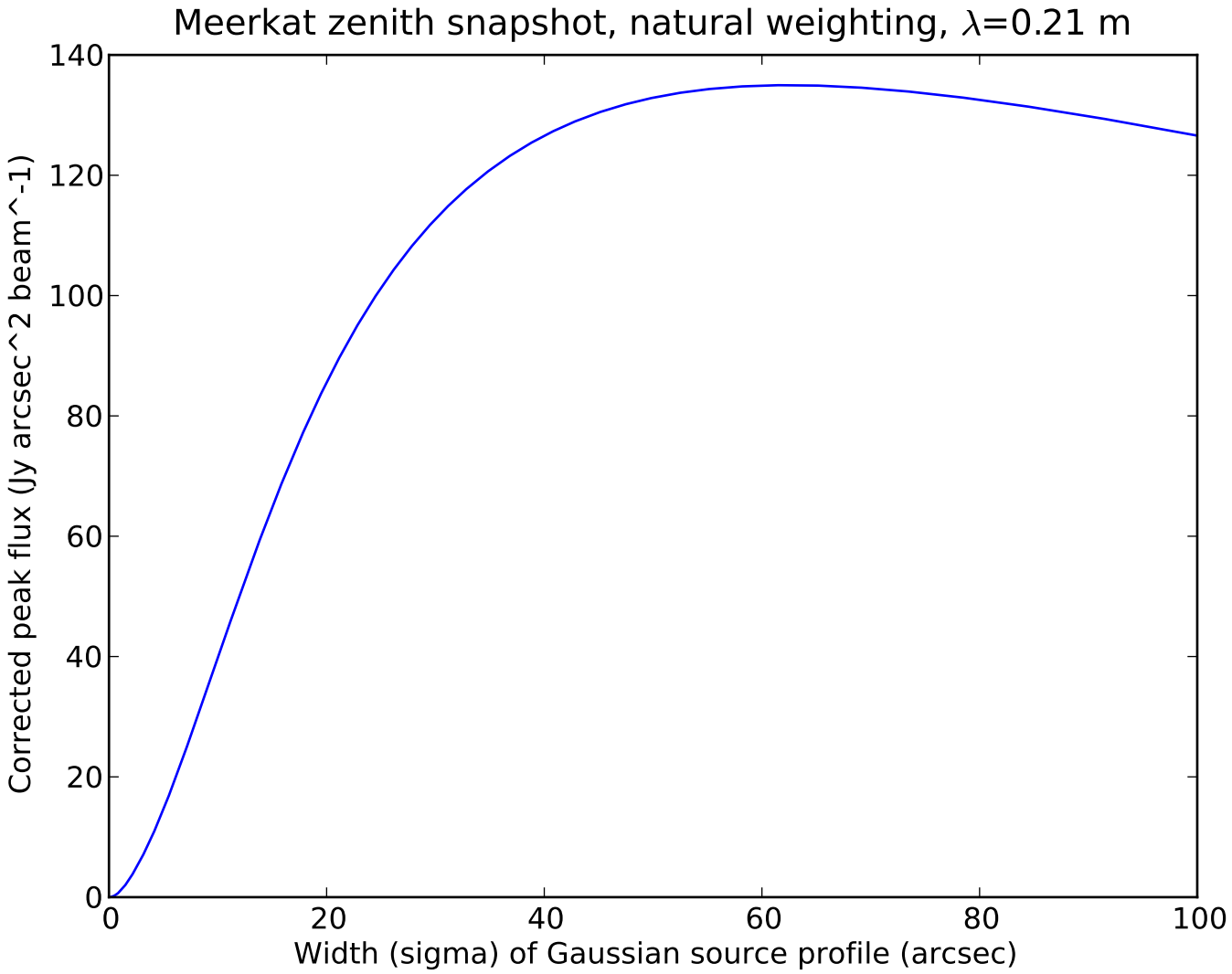


Figure 10: Source 'visibility' for natural weighting.